HHS Public Access

Author manuscript

Magn Reson Med. Author manuscript; available in PMC 2022 November 01.

Published in final edited form as:

Magn Reson Med. 2021 November ; 86(5): 2810–2821. doi:10.1002/mrm.28895.

Safety and imaging performance of two-channel RF shimming for fetal MRI at 3T

Filiz Yetisir[1], **Esra Abaci Turk**[1,2], **Bastien Guerin**[3,4], **Borjan A. Gagoski**[1,4], **P. Ellen Grant**[1,2,4], **Elfar Adalsteinsson**[5,6,7], **Lawrence L. Wald**[3,4,5]

[1]Fetal-Neonatal Neuroimaging & Developmental Science Center, Boston Children's Hospital, Boston, Massachusetts, USA

[2]Department of Pediatrics, Harvard Medical School, Boston, Massachusetts, USA

[3]Athinoula A. Martinos Center for Biomedical Imaging, Massachusetts General Hospital, Charlestown, Massachusetts, USA

[4]Department of Radiology, Harvard Medical School, Boston, Massachusetts, USA

[5]Harvard-MIT Division of Health Sciences and Technology, Cambridge, Massachusetts, USA

[6]Department of Electrical Engineering and Computer Science, Massachusetts Institute of Technology, Cambridge, Massachusetts, USA

[7]Institute for Medical Engineering and Science, Massachusetts Institute of Technology, Cambridge, Massachusetts, USA

Abstract

Purpose: This study investigates whether two-channel radiofrequency (RF) shimming can improve imaging without increasing specific absorption rate (SAR) for fetal MRI at 3T.

Methods: Transmit field $\left(B_1^+\right)$ average and variation in the fetus was simulated in seven numerical pregnant body models. Safety was quantified by maternal and fetal peak local SAR and fetal average SAR. The shim parameter space was divided into improved B_1^+ (magnitude and homogeneity) and improved SAR regions, and an overlap where RF shimming improved both classes of metrics compared with birdcage mode was assessed. Additionally, the effect of fetal position, tissue detail, and dielectric properties on transmit field and SAR was studied.

Results: A region of subject-specific RF shim parameter space improving both B_1^+ and SAR metrics was found for five of the seven models. Optimizing only B_1^+ metrics improved B_1^+ efficiency across models by 15% on average and 28% for the best-case model. B_1^+ variation improved by 26% on average and 49% for the best case. However, for these shim settings, fetal

Correspondence: Filiz Yetisir, Department of Newborn, Medicine, Boston Children's Hospital, 300 Longwood Avenue BCH 3181, Boston, MA 02115, USA. filiz.yetisir@childrens.harvard.edu.

SUPPORTING INFORMATION

Additional Supporting Information may be found online in the Supporting Information section.

SAR increased by up to 106%. The overlap region, where both B_1^+ and SAR metrics improve, showed an average B_1^+ efficiency improvement of 6% on average across models and 19% for the best-case model. B_1^+ variation improved by 13% on average and 40% for the best case. RFS could also decrease maternal/fetal SAR by up to 49%/58%.

Conclusion: RF shimming can improve imaging compared with birdcage mode without increasing fetal and maternal SAR when a patient-specific SAR model is incorporated into the shimming procedure.

Keywords

fetal magnetic resonance imaging (MRI); parallel transmission (pTx); pregnant body models; radiofrequency safety; radiofrequency (RF) shimming

1 | INTRODUCTION

MRI provides powerful structural and functional information on the fetus and placenta during pregnancy.[1–3] MR scanners operating at 3T have been increasingly used for fetal imaging due to improved signal-to-noise ratio (SNR) compared with 1.5T scanners, and, in some centers, due to scanner availability.[4,5] However, transmit radiofrequency (RF) field inhomogeneities, which cause flip angle (FA) variations, become more prominent at 3T, which results in degraded image quality.[6] The problem is especially acute during pregnancy because of the large abdominal size and high conductivity of the amniotic fluid. In addition, for the same imaging conditions, the specific absorption rate (SAR) can be greater at 3T than 1.5T. If regulatory limits are reached, image parameters such as repetition time (TR) and FA must be adjusted—further limiting imaging speed and image quality.[6] Although increased temperature, not SAR, is the primary health risk, SAR provides the energy source driving whole-body and localized tissue heating. SAR limitations are especially restrictive for fetal imaging as high SAR single-shot fast spin-echo sequences are routinely used to avoid fetal motion artifacts.[7] Thus, strategies to reduce transmit field inhomogeneities and SAR at 3T are needed.

Parallel transmission (pTx) technology[8–10] has the potential to mitigate transmit field inhomogeneities and reduce SAR for fetal MRI.[11–15] Several 3T scanners today are already equipped with two-channel pTx systems that are available for use with human subjects. The International Electrotechnical Commission (IEC) suggests limiting the whole-body average SAR (wbSAR) of the mother by 2 W/kg (normal operating mode), whereas no limits for local SAR exist for volume body transmit coils.[16] Using this wbSAR limitation in a conventional circularly polarized (CP) birdcage volume coil, local SAR values have been shown to be similar at 3T and 1.5T.[11,17] However, pTx can significantly increase local SAR exposure.[18] Even though several studies have investigated safety at 1.5T and 3T for conventional birdcage volume coils,[17,19–29] the safety of pTx for fetal MRI is understudied. RF shimming is a simplified form of pTx, where the complex weights of different transmit channels are optimized to improve image quality. Murbach et al. reported that two-channel RF shimming at 3T always increases fetal SAR and advised restriction to an excitation that

achieves the amplitude and phase relationship of the CP birdcage coils for pregnant women.[11] We refer to this RF shimming solution as the CP mode excitation. They investigated the SAR associated with the best shim settings for fetal B_1^+ efficiency and B_1^+ variation in three pregnant body models with different gestational ages (3, 7, and 9 months old) from the Virtual Population,[30,31] all artificially generated from the same nonpregnant female body model.

In this study, we build on the study by Murbach et al.[11] by extending the set of anatomical models to seven,[19] including the Virtual Population model of 7-month gestational age.[30,31] We also explicitly search for RF shim settings that provide improvement in B_1^+ efficiency and B_1^+ variation subject to the constraint that maternal or fetal SAR is not raised above the levels for the CP mode. Thus, we investigate whether two-channel RF shimming can improve imaging for fetal MRI at 3T without increasing maternal or fetal SAR. We investigate RF shimming with two channels as opposed to more channels because several 3T scanners today are equipped with a two-channel pTx system whereas higher channel pTx systems are not common. We also investigate the effect of the fetal position on imaging performance and safety by rotating the fetus by 20°, 160°, and 180° inside the uterus in one of the in-house pregnant body models.[19] Furthermore, we present a limited sensitivity study by altering the number of compartments in the maternal and fetal model, as well as the dielectric properties of amniotic fluid and fetal tissues in the Virtual Population model of 7-month gestational age.[30,31]

2 | METHODS

2.1 | Human body models

Figure 1 shows the body models used in this study. We employ five in-house pregnant body models (BCH1, BCH2, BCH3, BCH4-1-1, and BCH5) that were generated from MRI data of four pregnant women.[19] BCH2 has a twin pregnancy and BCH4-1-1 and BCH5 model the same subject positioned in the supine and left lateral postures, respectively. Four additional versions of BCH4-1-1[19] were also studied: BCH4-2-1 for which the arms in BCH4-1-1 were manually removed and BCH4-2-2, BCH4-2-3, and BCH4-2-4 for which, in addition to removing the arms in BCH4-1-1, the fetus was rotated inside the uterus by 20°, 160°, and 180°, respectively. We also used pregnant woman II (which we label PW_II) from the Virtual Population (IT'IS Foundation).[30,31] Supporting Information Figure S1 shows the transverse cross section of all body models. The transverse view emphasizes the approximate left to right symmetry in the supine models, which is less apparent in the cross sections of the two left-lateral models (BCH2 and BCH5).

2.2 | Electromagnetic simulations

All electromagnetic simulations were carried out for a two-channel 32-rung high-pass birdcage body coil, which is 450-mm long with a diameter of 714 mm (Figure 1) using Sim4Life (Zurich MedTech, Zurich, Switzerland). For a supine, head-first scanning position, channel 1 is driven at the head-posterior side and channel 2 at the head-left side of the subject. The coil was tuned (end ring capacitor values chosen) for the generic male body

model Duke from the Virtual Population to 123.2 MHz using a nonuniform rectangular discretization grid with a maximum resolution of 1.2 mm, 0.8 mm, and 2.5 mm and minimum resolution of 6.5 mm, 6.6 mm, and 18 mm in left-to-right, anterior-posterior (AP), and head-to-foot axes, respectively. The minimum resolution inside the body models was 3.5 mm (the BCH models have a native resolution of $2 \times 2 \times 2$ mm^3, and the Virtual Population model has a native resolution of $0.9 \times 0.9 \times 2$ mm^3 in torso). The same capacitor values and grid were used for all simulations. All finite-difference time-domain simulations in Sim4Life were run with a convergence criterion of −40 dB.

All models were simulated in the head-first position. All simulations were carried out such that the uterus is approximately centered in the coil on the head-to-foot axis as shown in Figure 1. All models were placed on approximately the same table position in the AP direction and approximately symmetrically with respect to the origin in the left-to-right direction. For PW_II, similar to Murbach et al.,[11] a minimal distance of 9 mm was ensured between the hips and arms to avoid RF loops.

2.3 | Tissue detail and dielectric properties

All maternal tissue dielectric properties were assigned according to the IT'IS database,[32,33] except amniotic fluid properties, which were assigned according to Peyman et al.[34] In BCH models, fetal brain and fetus (fetus except fetal brain) were assigned properties according to Hand et al.,[17] for which the tissue properties are age-adjusted based on the water content of the fetal tissues.[35] PW_II has 17 fetal tissues and more than 70 maternal tissues, whereas the BCH models have two fetal tissues (fetal brain and fetus) and 23–24 maternal tissues. Therefore, the effect of tissue detail on the SAR analysis was quantified by reassigning tissue properties in PW_II to reduce the total number of maternal and fetal tissues. First, PW_II was simulated in its original form, where fetal tissue properties were assigned age-adjusted values according to Wang et al.[35] Next, the fetus was made more homogeneous to have only fetal brain and fetus as in the BCH models. Then, both fetal and maternal tissues were reassigned to have a similar level of tissue detail as the BCH models. This version of PW_II was used when comparing imaging performance and SAR to BCH models. Note that in Murbach et al.,[11] adult tissue properties were assigned to fetal tissues and cerebrospinal fluid (CSF) properties were assigned to amniotic fluid. Therefore, for comparison, we also simulated PW_II with the same tissue assignments as in Murbach et al.[11] Finally, to quantify the effect of only fetal tissue properties (adult vs. age-adjusted) and only amniotic fluid properties, we simulated PW_II with age-adjusted fetal tissue properties, but amniotic fluid assigned to CSF.

2.4 | RF shimming

The electromagnetic simulation results of the two channels in the volume transmit coil were combined with differing phases and amplitude weights to simulate the parameter space of different RF shim settings. The relative amplitude between the channels was varied between 0 and 2 in steps of 0.1. The relative phase between the channels was varied from −90° to 270° in 10° increments. A relative amplitude of 1 and relative phase of 90° represents the CP mode excitation.

For each shim setting, the power was adjusted so that the maternal wbSAR is equal to 2 W/kg. For the truncated in-house body models, the total weight of the subject was used to calculate wbSAR. The 10 g averaged peak local SAR (pSAR10g) in the mother and fetus, as well as the average SAR (aveSAR) in the fetus, was calculated using the SAR calculation tool in Sim4Life. Additionally, the average value and the coefficient of variation (CV) of the transmit field magnitude ($\left|B_1^+\right|$) inside the fetus are calculated for each RF shim setting. Note that for the same maternal wbSAR, a lower $\left|B_1^+\right|$ CV means more uniform contrast and a higher average $\left|B_1^+\right|$ can translate into higher FA, or for a given FA, a shorter TR or better slice coverage. Hence, improving average $\left|B_1^+\right|$ and $\left|B_1^+\right|$ CV for the same maternal wbSAR improves imaging performance. For BCH2, which has a twin pregnancy, average $\left|B_1^+\right|$ and $\left|B_1^+\right|$ CV were calculated by treating both fetuses as a single region of interest (ROI). The fetal pSAR10g and fetal aveSAR were calculated by taking the maxima among the two fetuses for each shim setting. The relative phase range of −90° to 270° covers all shim possibilities; however, the relative amplitude range does not (it can go up above 2). Therefore, we also computed the worst-case shim settings for maternal pSAR10g, fetal pSAR10g, and fetal aveSAR using the maximum generalized eigenvalue analysis[18] on the Q matrices.[9,36]

For each pregnant body model, we divided the shim parameter space into an improved imaging performance region with higher average $\left|B_1^+\right|$ and lower $\left|B_1^+\right|$ CV compared with CP mode, and improved SAR regions, where each SAR metric (maternal pSAR10g, fetal pSAR10g, and fetal aveSAR) is improved compared with CP mode. Then, we assessed the "AND-ed" overlap of these regions, where both $\left|B_1^+\right|$ and SAR metrics are improved compared with CP mode.

3 | RESULTS

Figure 2 plots the imaging performance metrics (average $\left|B_1^+\right|$ and $\left|B_1^+\right|$ CV) over the parameter space for each pregnant body model. The CP mode is marked by a purple dot at the center. The improved imaging performance region is shown by the red-dashed region. The optimal operating point for each imaging performance metric, average $\left|B_1^+\right|$ and $\left|B_1^+\right|$ CV, is marked by a red triangle and star, respectively. The region where both imaging performance and all SAR metrics improve compared with CP mode is shown by the black-dashed region. A black triangle or star marks the position of best imaging performance (measured by average $\left|B_1^+\right|$ or $\left|B_1^+\right|$ CV) inside the black-dashed region.

The overall patterns of imaging performance metrics across the RF shimming space in Figure 2 are similar among supine body models for which the improved imaging region (red-dashed region) is mostly located on the right side of the shim space. In contrast, for the two left lateral body models, the good shimming region is roughly symmetrical around the center of the shim space. Thus, the optimal shim settings are located close to the CP mode

for the two left lateral models, whereas they are always located on the right side of the shim space for the supine models.

Figure 3 shows the SAR metrics (maternal pSAR10g, fetal pSAR10g, and fetal aveSAR) across the RF shim parameter space for different pregnant body models. Again, the improved imaging performance region is shown by the red-dashed region; the region of improvement in both imaging performance and all SAR metrics is shown by the black-dashed region. In addition, a pink-dashed region shows where each individual SAR metric is improved compared with CP mode (regardless of imaging performance). These improved SAR regions for individual SAR metrics highlight that, similar to previous findings,[11] maternal pSAR10g and fetal SAR have roughly opposite patterns, ie, shim settings that decrease maternal pSAR10g usually increase fetal pSAR10g and fetal aveSAR and vice versa.

Figure 3 also shows the location of the worst-case shim settings (gray square) for each SAR metric. For supine models, maternal pSAR10g worst-case shim setting always has a relative amplitude ≥1.9, whereas fetal pSAR10g and fetal aveSAR worst-case shim settings always have a relative amplitude ≤0.8 and ≤0.4, respectively. Left lateral models have less regular fetal and maternal SAR patterns that are different from those of supine models, as can be seen in Figure 3. The worst-case shim settings for left lateral models have relative amplitudes varying between 1.0 and 3.0 for maternal pSAR10g and between 0.9 and 4.5 for fetal SAR. See Supporting Information Table S1 and Figure S2 for the worst-case shim settings of each model.

Figure 4 shows the best improvement possible in either average $|B_1^+|$ or $|B_1^+|$ CV with or without increasing maternal or fetal SAR compared with CP mode across various pregnant models. Purple, red, and black bars in Figure 4 correspond to the purple dot (CP mode), red triangles/stars (optimal average $|B_1^+|/|B_1^+|$ CV without SAR restrictions), and black triangles/stars (optimal average $|B_1^+|/|B_1^+|$ CV that also improves all SAR metrics) in Figure 2, respectively. When only B_1^+ metrics are optimized (no SAR constraints), RF shimming can improve average $|B_1^+|$ by 15% on average across all body models and 28% for the best-case model (purple bars vs red bars in Figure 4, top). B_1^+ variation can be improved by 26% on average across all body models and 49% for the best-case model (purple bars vs red bars in Figure 4, bottom). When both maternal and fetal SAR is constrained to be less than the corresponding CP mode values, RF shimming can improve average $|B_1^+|$ by 6% on average across all body models and by 19% for the best-case model (purple bars vs black bars in Figure 4, top). $|B_1^+|$ variation can be improved by 13% on average across all models and by 40% for the best-case model (purple bars vs black bars in Figure 4, bottom).

In Figure 5, maternal and fetal SAR is compared across models for CP mode, shim settings that improve imaging performance, and worst-case shim settings. Among all shim settings that improve imaging performance (red-shaded region in Figure 5), maternal pSAR10g, fetal pSAR10g, and fetal aveSAR can increase by up to 37%, 38%, and 168%, respectively,

compared with CP mode. For the shim settings that optimize average $|B_1^+|$ and $|B_1^+|$ CV (red triangles and stars in Figure 5), maternal pSAR10g, fetal pSAR10g, and fetal aveSAR can increase by up to 26%, 26%, and 106%, respectively, compared with CP mode. On the other hand, RF shimming can also decrease maternal pSAR10g, fetal pSAR10g, or fetal aveSAR by up to 49%, 58%, or 49%, respectively, compared with CP mode, while still improving imaging performance (bottom boundary of the red-shaded region in Figure 5). Across all body models, maternal pSAR10g, fetal pSAR10g, and fetal aveSAR can reach 53 W/kg, 23 W/kg, and 7.2 W/kg, respectively, for the worst-case among all shim settings, compared with 44 W/kg, 19 W/kg, and 4.3 W/kg for the CP mode.

3.1 | Fetal position

Figure 6 shows the effect of rotating the fetus inside the uterus of model BCH-4-2-1 by 20° (BCH4-2-2), 160° (BCH4-2-3), and 180° (BCH4-2-4) around the z-axis on maternal and fetal SAR, as well as average $|B_1^+|$ and $|B_1^+|$ CV. Maternal pSAR10g is only mildly affected by fetal rotation (<3%). Maximum changes in the other metrics, fetal pSAR10g, fetal aveSAR, average $|B_1^+|$ and $|B_1^+|$ CV, were 13%, 32%, 2%, and 11% for the CP mode and 16%, 39%, 11%, and 31% for RF shim settings in the improved imaging performance region. For the worst-case SAR values, the effect of the rotation was smaller; fetal pSAR10g and fetal aveSAR changed by up to 4% and 9%, respectively. The fetal position did not significantly change the worst-case shim settings for maternal SAR, whereas it changed worst-case shim settings for fetal aveSAR the most (relative amplitude changed from 0.4 to 0.1 and relative phase changed from 230° to 0°, see Supporting Information Table S1). Supporting Information Figure S3 depicts the comparison of the patterns of imaging performance and SAR metrics in the RF shim parameter space for all four models.

3.2 | Tissue detail and dielectric properties

Table 1 shows the effect of different alterations to tissue detail and dielectric properties in model PW_II. The alterations included assigning different dielectric properties to fetal tissues and amniotic fluid, as well as simplification of fetal and maternal tissues. The effects of these factors are shown for the CP mode, worst-case shim settings, and RF shim settings that improve imaging performance (average $|B_1^+|$ and $|B_1^+|$ CV). For reference, the first row shows SAR metrics for this model reported in Murbach et al.[11] The second row reports SAR values when tissue assignments in Murbach et al.[11] are replicated in our simulations. Maternal and fetal SAR values for the CP mode or the worst-case shim settings using our body coil are at most 16% different from those reported in Murbach et al.,[11] who modeled a different body coil. Subsequent rows alter the model PW_II one aspect at a time. Row 4 represents the most realistic model in that it has full tissue classes and the most relevant dielectric property assignments. Compared with row 4, our replication of the Murbach et al.[11] case (row 2) resulted in fetal SAR overestimation and underestimation of up to 35% and 34%, respectively. Row 3 assigns the amniotic fluid property to that of CSF instead of Peyman et al.,[34] which resulted in fetal SAR overestimation and underestimation of up to 14% and 11%, respectively, compared with row 4. Row 5 reduces the number of fetal tissues to 2, which resulted in fetal SAR overestimation and underestimation of up to 25% and 18%,

respectively, compared with row 4. Row 6 additionally reduces the number of maternal tissues to 25, which resulted in fetal SAR overestimation and underestimation of up to 14% and 22%, respectively, compared with row 4. Simplification of maternal and fetal tissues, changing dielectric properties of fetal tissues or the amniotic fluid results in overestimation and underestimation of maternal pSAR10g by 8% and 4%, respectively, compared with row 4.

4 | DISCUSSION

We investigated whether two-channel RF shimming can improve imaging performance for fetal MRI without increasing the fetal or maternal SAR using a diverse set of anatomically realistic pregnant body models. For different shim settings all normalized to a maternal wbSAR of 2 W/kg, we quantified improvements in transmit field efficiency (average $|B_1^+|$) and transmit field uniformity ($|B_1^+|$ CV) and assessed maternal pSAR10g, fetal pSAR10g, and fetal aveSAR.

In a previous study, Murbach et al.[11] concluded that fetal SAR always increases with RF shimming compared with CP mode and advised restriction to CP mode for pregnant women. They reached this conclusion by investigating the SAR associated with only the optimal shim settings for B_1^+ efficiency and B_1^+ variation. In this study, in five of the seven body models assessed, we could find a shim setting that improves both the two imaging metrics and the three SAR metrics assessed compared with the CP mode excitation (Figure 2, black triangles and stars). However, this usually required shim settings different from the shim settings obtained when B_1^+ metrics were optimized alone. In one of the body models used by Murbach et al.,[11] PW_II, we found that RF shimming (using our coil) can improve average $|B_1^+|$ and $|B_1^+|$ CV by up to 3% and 14%, respectively, without increasing maternal or fetal SAR compared with CP mode.

We observed a large variation in imaging performance improvement with RF shimming over the CP mode among different pregnant models (Figure 4). Without increasing any of the SAR metrics, the best improvement in average $|B_1^+|$ (19%) was observed for the high BMI model BCH1 (BMI = 42.4). The best improvement in $|B_1^+|$ CV (40%) was observed for BCH4-1-1 (supine, arms on side). For BCH4-2-1, shim settings that improved imaging performance resulted in either higher fetal aveSAR (almost all shim settings) or higher maternal pSAR10g (some shim settings) compared with CP mode. For BCH5 (left lateral), RF shimming could only marginally improve imaging performance, even without SAR penalties. For BCH2 (left lateral), all shim settings that improved imaging performance also increased maternal pSAR10g compared with CP mode. Across all seven models, RF shimming improved average $|B_1^+|$ by 6% on average and $|B_1^+|$ CV by 13% on average without increasing maternal or fetal SAR compared with CP mode.

Similar to the findings of Murbach et al.,[11] we found that RF shimming, while improving imaging performance, can also significantly increase fetal SAR when SAR penalties are not

applied. Fetal SAR increases by up to 168% were seen among shim settings that improve imaging performance and by up to 106% for shim settings that optimize the imaging metrics. For the shim settings that optimize B_1^+ efficiency and uniformity, fetal pSAR10g increased for two of seven models (BCH4-2-1 and PW_II), fetal aveSAR increased for six of seven models (all except BCH2), and maternal pSAR10g increased for two of seven models (BCH2 and BCH4-2-1) compared with CP mode. Therefore, fetal aveSAR was usually the limiting factor in improving imaging performance with RF shimming without increasing SAR compared with CP mode. On the other hand, it was also possible to find shim settings that decrease maternal pSAR10g, fetal pSAR10g, and fetal aveSAR (by up to 49%, 58%, and 49%, respectively), while still improving imaging performance compared with the CP mode (Figure 5).

We have shown that RF shimming can improve imaging performance in fetal MRI without increasing maternal or fetal SAR. However, achieving this goal might require subject-specific SAR modeling, which is currently not practical for pregnant women. Progress toward subject-specific SAR models generated rapidly at the scanner has been made for nonpregnant patients.[37,38] These approaches might be tailored to pregnant women in the future. In addition, improvements in imaging performance using two-channel RF shimming are limited even without SAR considerations (15% improvement in average $|B_1^+|$ and 26% improvement in $|B_1^+|$ CV on average across all models). Increasing the number of transmit channels in the hardware and utilizing full pTx where different RF waveforms rather than only different complex weights are applied to each channel could result in better improvements in both B_1^+ and SAR.[39–41]

In this study, we used two models generated from the same subject positioned in two postures. For the models included in this study, the left lateral posture (BCH5) was more optimal than head-first supine posture (BCH4-1-1) in terms of average $|B_1^+|$ and $|B_1^+|$ CV, both in CP mode and with RF shimming (Figure 4). In addition, shim settings that optimize B_1^+ metrics for both left lateral models in this study (BCH2 and BCH5) were in close vicinity of the CP mode (relative amplitude of 1 and relative phase of 90°). In contrast, the shim settings which optimize B_1^+ metrics for the supine models were located on the right half of the RF shim parameter space (relative phase between 90° and 270°). This distinction between the two postures is likely due to the different shapes of the pregnant abdomen in these two postures as shown in Supporting Information Figure S1. These observations motivate generating more left lateral body models in the future to investigate whether left lateral posture could be in general advantageous compared with supine posture from an excitation perspective and whether subject positioning can address part of the transmit efficiency and uniformity issues in CP mode without using RF shimming.

Due to a lack of local SAR limits in regulatory guidelines for body transmit coils, we use the CP mode maternal and fetal SAR values for each model as a standard for comparison. Although this makes sense for comparing a new methodology such as RF shimming to the “standard” (CP mode operation), it also means that models with lower CP mode SAR values

are potentially overly restricted in the RF shimming mode. As the temperature is the direct measure of safety, rather than SAR, temperature simulations[11,17] could be used to determine SAR limits that are globally safe across different models in RF shimming mode. This might relax the SAR constraints for models with low CP mode SAR values, increasing the overall imaging performance improvement by RF shimming across the pregnant population.

We found that across all models, maternal pSAR10g, fetal pSAR10g, and fetal aveSAR can reach 44 W/kg, 19 W/kg, and 4.3 W/kg, respectively, for CP mode and 53 W/kg, 23 W/kg, and 7.2 W/kg, respectively, for the worst-case shim settings. All SAR values reported in this study were calculated for the normal operating mode (maternal wbSAR = 2 W/kg), which is the operating mode suggested by the IEC[16] for pregnant women. However, in practice, wbSAR of the mother does not stay at 2 W/kg throughout the whole examination, which is what is assumed in this study. In our previous study,[19] we showed that in a typical realistic fetal examination of approximately 1 hour in CP mode, the time-averaged maternal wbSAR was approximately 0.7 W/kg when the variations from different sequences are accounted for, as well as the scan prescription periods with zero SAR. In this case, the time-averaged maternal pSAR10g, fetal pSAR10g, and fetal aveSAR values would be up to 15 W/kg, 6.7 W/kg, and 1.5 W/kg for CP mode and 18.6 W/kg, 8.1 W/kg, and 2.5 W/kg for worst-case RF shimming scenarios. On the other hand, temperature, not SAR, is the most relevant parameter when considering safety. The maximum temperature increase during a specific examination depends on the exact time course of RF exposure and is not necessarily well characterized by the time-averaged SAR. Therefore, the use of SAR-intensive sequences (maternal wbSAR = 2 W/kg) for a long period, in a way that considerably deviates from current practice in CP mode, should be approached with care as it may lead to excessive tissue heating.

We observed a high intersubject variability of maternal and fetal SAR (up to a factor of 2.4) in the CP mode, in agreement with our previous study.[19] Using RF shimming, this variability increased further (up to a factor of 4.4). Several factors likely contributed to this variability, including maternal BMI, maternal posture that changes maternal body shape, maternal arms' position, amniotic fluid distribution inside the uterus, and gestational age—which affects the size of the fetus as well as the amount of amniotic fluid. We previously showed[19] that there is a positive linear relationship between maternal pSAR10g in the trunk and maternal BMI in CP mode. In addition, in CP mode, fetal pSAR10g was lower ($P < .05$) when the arms of the mother are positioned at the side compared with upwards or when the mother was positioned left laterally compared with supine.[19] Murbach et al.[11] showed that constrictions of amniotic fluid between regions can lead to a pronounced hotspot. A few studies[11,26,27] assessing the effect of gestational age on fetal SAR showed a significant variation of fetal SAR with gestational age (up to a factor of approximately 5).

In-house models used in this study had a lower number of maternal and fetal tissues compared with the commercial IT'IS model, PW_II. Therefore, we studied the effect of tissue detail on maternal and fetal SAR. Simplification of maternal and fetal tissues in PW_II to a similar level as the BCH models resulted in up to 22% underestimation and 7% overestimation of fetal pSAR10g, up to 14% overestimation of fetal aveSAR, and up to 4% underestimation and 8% overestimation of maternal pSAR10g. Note that these variations

based on tissue detail level are much less than the intersubject variation of fetal and maternal SAR (up to a factor of 2.4 for CP mode and 4.4 for RFS). This result echoes a similar study in nonpregnant patients.[37] In addition, we found that rotating the fetus by 20°, 160°, or 180° changed fetal SAR by up to 39%, and fetal B_1^+ by up to 31% for RF shimming. These findings support the need for more patient-specific pregnant models to assess RF safety in the pregnant population.

Because the in-house models were derived from pregnant patients' scans, their extent along the superior-inferior direction was limited (i.e., they are cropped) compared with the commercial model PW_II, which was artificially generated from a nonpregnant female model. However, all BCH models extended above and below the coil by at least 15% of the coil length except BCH3, where the model extended beyond the coil by 8% (37 mm) and 49% (225 mm) in the head and foot directions, respectively. For the full-body model PW_II, the power loss outside this range constituted 8% of the total absorbed power. Hence, using truncated body models is likely to result in a small overestimation of fetal and maternal SAR.

We used average $\left|B_1^+\right|$ and $\left|B_1^+\right|$ CV inside the entire fetus as our imaging performance metrics. The results might change if the ROI is changed, for instance, into the fetal brain only. However, this reduction in the volume of the ROI may increase the dependence of imaging performance metrics on the fetal positioning inside the uterus. Hence, for simplicity and consistency with Murbach et al.,[11] we used the entire fetus as our ROI.

In this study, we only investigated a fetus/uterus-centered imaging landmark. Murbach et al.[11] investigated five imaging landmarks along the z-axis (head to foot). Except for one case (a short coil of 400-mm length), the fetus-centered imaging landmark was found to result in the highest SAR exposure for the fetus. Additionally, we used a single coil model with realistic dimensions.[11] However, the type, geometry, and the dimensions of the coil are likely to affect the resulting maternal and fetal SAR values. Murbach et al.[11] found that maternal and fetal SAR decreased when the coil length was increased or the coil diameter was decreased, and they increased when the coil length was decreased (12% increase in worst-case fetal pSAR10g). Moreover, the model we call PW_II is found in both our work and that of Murbach et al.[11] with the same tissue-property assignments, thus allowing a direct bridge to other coils. Note that our coil (32-rung, high-pass birdcage, 450-mm length, 714-mm diameter) differs from the reference coil used in Murbach et al.[11] (16-rung, band-pass birdcage, 480-mm length, 750-mm diameter). We found that the maternal and fetal SAR in the CP mode and the worst-case scenario using our coil were at most 16% different than those of the reference coil reported by Murbach et al.[11] (Table 1).

5 | CONCLUSION

Several 3T scanners today are equipped with two-channel pTx systems that are available for use with pregnant patients. We investigated the potential of two-channel RF shimming to improve the transmit field efficiency and uniformity for fetal MRI at 3T. We also studied the implications of using RF shimming on maternal and fetal safety. We found that even though

RF shimming can significantly increase both maternal and fetal SAR compared with the standard mode of excitation, the CP mode, careful SAR management using subject-specific pregnant body models could allow it to improve imaging performance without increasing the SAR load on the fetus or the mother. Currently, subject-specific SAR management is not practical for pregnant women. However, progress toward rapid subject-specific SAR model generation has been made for nonpregnant patients, which may be tailored to pregnant women in the future.

Supplementary Material

Refer to Web version on PubMed Central for supplementary material.

ACKNOWLEDGMENTS

This work was supported by National Institutes of Health grants R01EB017337, U01HD087211, R01EB006847 and R01HD100009.

REFERENCES

1. Bulas D, Egloff A. Benefits and risks of MRI in pregnancy. Semin Perinatol. 2013;37:301–304. [PubMed: 24176150]
2. Pugash D, Brugger PC, Bettelheim D, Prayer D. Prenatal ultra-sound and fetal MRI: the comparative value of each modality in prenatal diagnosis. Eur J Radiol. 2008;68:214–226. [PubMed: 18790583]
3. American College of Radiology, Society for Pediatric Radiology. ACR–SPR Practice Parameter for the Safe and Optimal Performance of Fetal Magnetic Resonance Imaging (MRI). Published 2010. Accessed April 11, 2021. Reston, VA: American College of Radiology, Society of Pediatric Radiology. https://www.acr.org/-/media/ACR/Files/Practice-Parameters/mr-fetal.pdf
4. Krishnamurthy U, Neelavalli J, Mody S, et al. MR imaging of the fetal brain at 1.5T and 3.0T field strengths: comparing specific absorption rate (SAR) and image quality. J Perinat Med. 2015;43:209–220. [PubMed: 25324440]
5. Victoria T, Johnson AM, Edgar JC, Zarnow DM, Vossough A, Jaramillo D. Comparison between 1.5-T and 3-T MRI for fetal imaging: is there an advantage to imaging with a higher field strength? AJR Am J Roentgenol. 2016;206:195–201. [PubMed: 26700352]
6. Soher BJ, Dale BM, Merkle EM. A review of MR physics: 3T versus 1.5T. Magn Reson Imaging Clin N Am. 2007;15:277–290, v. [PubMed: 17893049]
7. Yamashita Y, Namimoto T, Abe Y, et al. MR imaging of the fetus by a HASTE sequence. AJR Am J Roentgenol. 1997;168:513–519. [PubMed: 9016238]
8. Katscher U, Börnert P, Leussler C, van den Brink JS. Transmit SENSE. Magn Reson Med. 2003;49:144–150. [PubMed: 12509830]
9. Zhu Y Parallel excitation with an array of transmit coils. Magn Reson Med. 2004;51:775–784. [PubMed: 15065251]
10. Adriany G, Van de Moortele P-F, Wiesinger F, et al. Transmit and receive transmission line arrays for 7 Tesla parallel imaging. Magn Reson Med. 2005;53:434–445. [PubMed: 15678527]
11. Murbach M, Neufeld E, Samaras T, et al. Pregnant women models analyzed for RF exposure and temperature increase in 3T RF shimmed birdcages. Magn Reson Med. 2017;77:2048–2056. [PubMed: 27174499]
12. Murbach M, Neufeld E, Cabot E, et al. Anatomical models of pregnant women in 3T pTx body coils: evaluation of SAR and B1+ optimization in various imaging positions. In: Proceedings of the 23rd Annual Meeting of ISMRM, Toronto, Ontario, Canada, 2015. p. 3216.
13. Yetisir F, Turk EA, Guerin B, Grant EP, Wald LL, Adalsteinsson E. Potential of parallel transmission for fetal imaging in reducing SAR and mitigating flip angle inhomogeneities: a

simulation study at 3T. In: Proceedings of the 25th Annual Meeting of ISMRM, Honolulu, HI, USA, 2017, p. 4823.

14. Filippi C, Johnson A, Nickerson J, Sussman B, Gonyea J, Andrews T. Fetal imaging with multitransmit MR at 3.0T: preliminary findings. In: Proceedings of the 18th Annual Meeting of ISMRM, Stockholm, Sweden, 2010, p. 2023.
15. Brink WM, Gulani V, Webb AG. Clinical applications of dual-channel transmit MRI: a review: clinical applications of dual-channel transmit MRI. J Magn Reson Imaging. 2015;42:855–869. [PubMed: 25854179]
16. International Electrotechnical Commission. IEC 60601-2-33: Medical electrical equipment-P articular requirements for the basic safety and essential performance of magnetic resonance equipment for medical diagnosis. https://webstore.iec.ch/publication/22705. Published 2010. Updated 2015. Accessed April 22, 2021.
17. Hand JW, Li Y, Hajnal JV. Numerical study of RF exposure and the resulting temperature rise in the foetus during a magnetic resonance procedure. Phys Med Biol. 2010;55:913–930. [PubMed: 20090188]
18. Murbach M, Neufeld E, Cabot E, et al. Virtual population-based assessment of the impact of 3 Tesla radiofrequency shimming and thermoregulation on safety and B1+ uniformity. Magn Reson Med. 2016;76:986–997. [PubMed: 26400841]
19. Abaci Turk E, Yetisir F, Adalsteinsson E, et al. Individual variation in simulated fetal SAR assessed in multiple body models. Magn Reson Med. 2020;83:1418–1428. [PubMed: 31626373]
20. Murbach M, Cabot E, Neufeld E, et al. Local SAR enhancements in anatomically correct children and adult models as a function of position within 1.5 T MR body coil. Prog Biophys Mol Biol. 2011;107:428–433. [PubMed: 21964524]
21. Hand JW, Li Y, Thomas EL, Rutherford MA, Hajnal JV. Prediction of specific absorption rate in mother and fetus associated with MRI examinations during pregnancy. Magn Reson Med. 2006;55:883–893. [PubMed: 16508913]
22. Luo M, Hu C, Zhuang Y, Chen W, Liu F, Xin SX. Numerical assessment of the reduction of specific absorption rate by adding high dielectric materials for fetus MRI at 3 T. Biomed Eng Biomed Tech. 2016;61:455–461.
23. Kikuchi S, Saito K, Takahashi M, Ito K. Temperature elevation in the fetus from electromagnetic exposure during magnetic resonance imaging. Phys Med Biol. 2010;55:2411–2426. [PubMed: 20360633]
24. Pediaditis M, Leitgeb N, Cech R. RF-EMF exposure of fetus and mother during magnetic resonance imaging. Phys Med Biol. 2008;53:7187–7195. [PubMed: 19033645]
25. Gowland PA, Wilde JD. Temperature increase in the fetus due to radio frequency exposure during magnetic resonance scanning. Phys Med Biol. 2008;53:L15–L18. [PubMed: 18843171]
26. Wu D, Shamsi S, Chen J, Kainz W. Evaluations of specific absorption rate and temperature increase within pregnant female models in magnetic resonance imaging birdcage coils. IEEE Trans Microw Theory Tech. 2006;54:4472–4478.
27. Wang Z, Yeo D, Xu G, Jin J, Robb FJ. SAR evaluation of whole-body pregnant woman models at different gestational stage and position in MRI birdcage coil. In: Proceedings of the 18th Annual Meeting of ISMRM, Stockholm, Sweden, 2010, p. 3878.
28. Saito K, Kikuchi S, Takahashi M, Ito K, Ikehira H. SAR estimations of pregnant woman during MR imaging for abdomen by numerical calculations. In: Proceedings of 2007 18th International Zurich Symposium on Electromagnetic Compatibility, 2007, pp. 45–48.
29. Shamsi S, Wu DG, Chen J, Liu R, Kainz W. SAR evaluation of pregnant woman models in 64 MHz MRI birdcage coil. In Proceedings of 2006 IEEE MTT-S International Microwave Symposium Digest, 2006, pp. 225–228.
30. Christ A, Kainz W, Hahn EG, et al. The Virtual Family—development of surface-based anatomical models of two adults and two children for dosimetric simulations. Phys Med Biol. 2010;55:N23–N38. [PubMed: 20019402]
31. Gosselin M-C, Neufeld E, Moser H, et al. Development of a new generation of high-resolution anatomical models for medical device evaluation: the Virtual Population 3.0. Phys Med Biol. 2014;59:5287–5303. [PubMed: 25144615]

32. Hasgall PA, Di Gennaro F, Baumgartner C, et al. IT'IS Database for Thermal and Electromagnetic Parameters of Biological Tissues. Version 4.0, 5 15, 2018. Zurich: IT'IS Foundation. DOI: 10.13099/VIP21000-04-0. itis.swiss/database.

33. Gabriel S, Lau RW, Gabriel C. The dielectric properties of biological tissues: II. Measurements in the frequency range 10 Hz to 20 GHz. Phys Med Biol. 1996;41:2251–2269. [PubMed: 8938025]

34. Peyman A, Gabriel C, Benedickter HR, Fröhlich J. Dielectric properties of human placenta, umbilical cord and amniotic fluid. Phys Med Biol. 2011;56:N93–N98. [PubMed: 21364261]

35. Wang J, Fujiwara O, Watanabe S. Approximation of aging effect on dielectric tissue properties for SAR assessment of mobile telephones. IEEE Trans Electromagn Compat. 2006;48:408–413.

36. Graesslin I, Homann H, Biederer S, et al. A specific absorption rate prediction concept for parallel transmission MR. Magn Reson Med. 2012;68:1664–1674. [PubMed: 22231647]

37. Milshteyn E, Guryev G, Torrado-Carvajal A, et al. Individualized SAR calculations using computer vision-based MR segmentation and a fast electromagnetic solver. Magn Reson Med. 2021;85:429–443. [PubMed: 32643152]

38. Meliadò EF, Raaijmakers A, Sbrizzi A, et al. A deep learning method for image-b ased subject-specific local SAR assessment. Magn Reson Med. 2020;83:695–711. [PubMed: 31483521]

39. Guérin B, Gebhardt M, Serano P, et al. Comparison of simulated parallel transmit body arrays at 3 T using excitation uniformity, global SAR, local SAR, and power efficiency metrics. Magn Reson Med. 2015;73:1137–1150. [PubMed: 24752979]

40. Wu X, Zhang X, Tian J, et al. Comparison of RF body coils for MRI at 3 T: a simulation study using parallel transmission on various anatomical targets. NMR Biomed. 2015;28:1332–1344. [PubMed: 26332290]

41. Tian J, DelaBarre L, Strupp J, et al. Searching for the optimal body coil design for 3T MRI. In: Proceedings of the 21st Annual Meeting of ISMRM, Salt Lake City, Utah, USA, 2013. p. 2746.

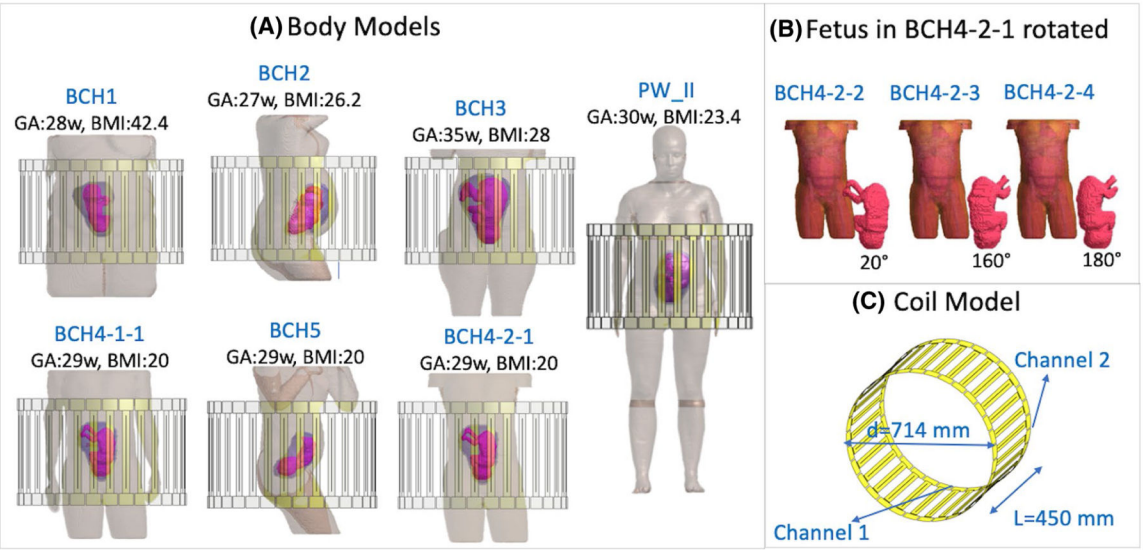

FIGURE 1.

The numerical pregnant body models (A,B) and the numerical model of the two-channel, 32-rung high pass birdcage coil (C) used in this study. BCH2 has twin pregnancy. BCH4 and BCH5 are generated from the same pregnant woman scanned in supine and left lateral postures, respectively. BCH4-2-1, BCH4-2-2, BCH4-2-3, and BCH4-2-4 are manually generated from BCH4-1-1 by removing the arms and by removing the arms and rotating the fetus by 20°, 160°, and 180°, respectively. BMI, body mass index; GA, gestational age; w, weeks

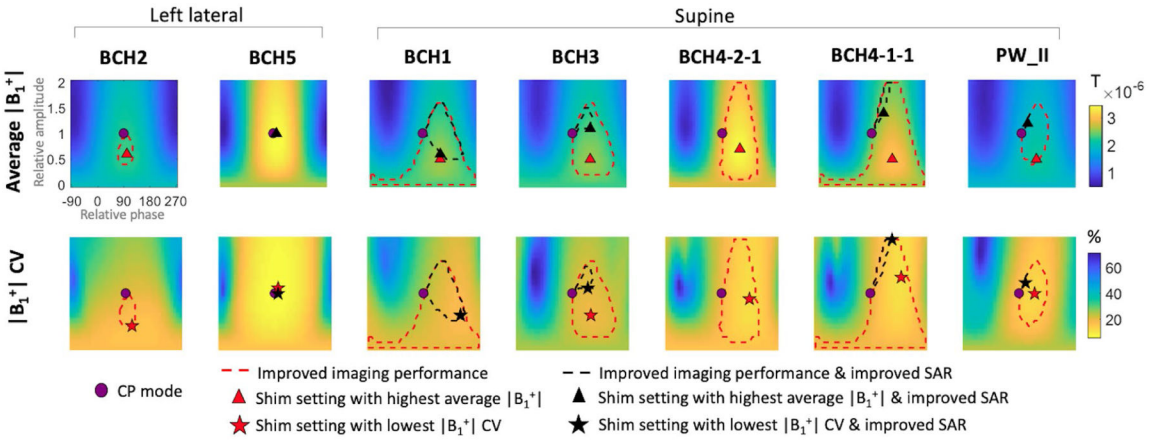

FIGURE 2.

Average and coefficient of variation (CV) of the transmit field magnitude $\left(\left|B_1^+\right|\right)$ inside the fetus for different RF shim settings, where the relative amplitude and relative phase of the two channels are varied from 0 to 2 (vertical axis) and −90° to 270° (horizontal axis), respectively. All shim settings are normalized to a maternal whole-body average SAR (wbSAR) of 2 W/kg. CP mode: circularly polarized birdcage mode, improved imaging performance: both average $\left|B_1^+\right|$ and $\left|B_1^+\right|$ CV are improved compared with CP mode, improved SAR: all three SAR metrics (maternal pSAR10g, fetal pSAR10g, and fetal aveSAR) are less than CP mode values of the corresponding body model

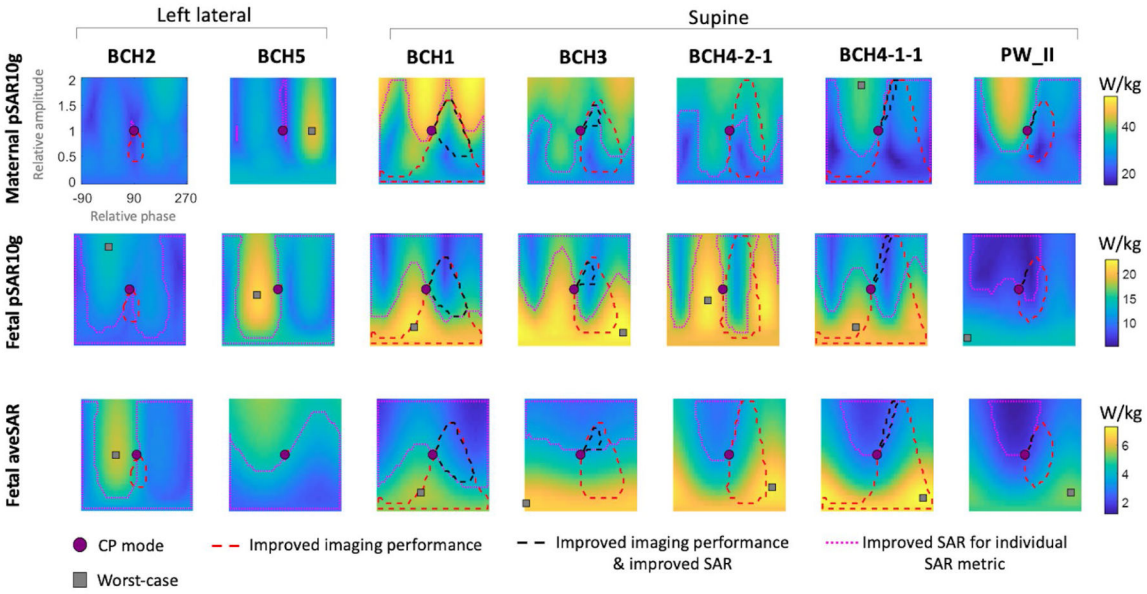

FIGURE 3.

Maternal and fetal peak local SAR (pSAR10g) and fetal average SAR (aveSAR) for different RF shim settings where the relative amplitude and relative phase of the two channels are varied from 0 to 2 (vertical axis) and −90° to 270° (horizontal axis), respectively. All shim settings are normalized to a maternal whole-body average SAR (wbSAR) of 2 W/kg. CP mode: circularly polarized birdcage mode, improved imaging performance: both average $|B_1^+|$ and $|B_1^+|$ CV are improved compared with CP mode, improved SAR: all three SAR metrics (maternal pSAR10g, fetal pSAR10g, and fetal aveSAR) are less than the CP mode values of the corresponding body model, improved SAR for individual SAR metric: the individual SAR metric in each subplot is lower than its corresponding CP mode value, worst-case: RF shim setting that maximizes an individual SAR metric. For some cases, the worst-case shim setting has a relative amplitude >2; hence, it is not shown on the plot

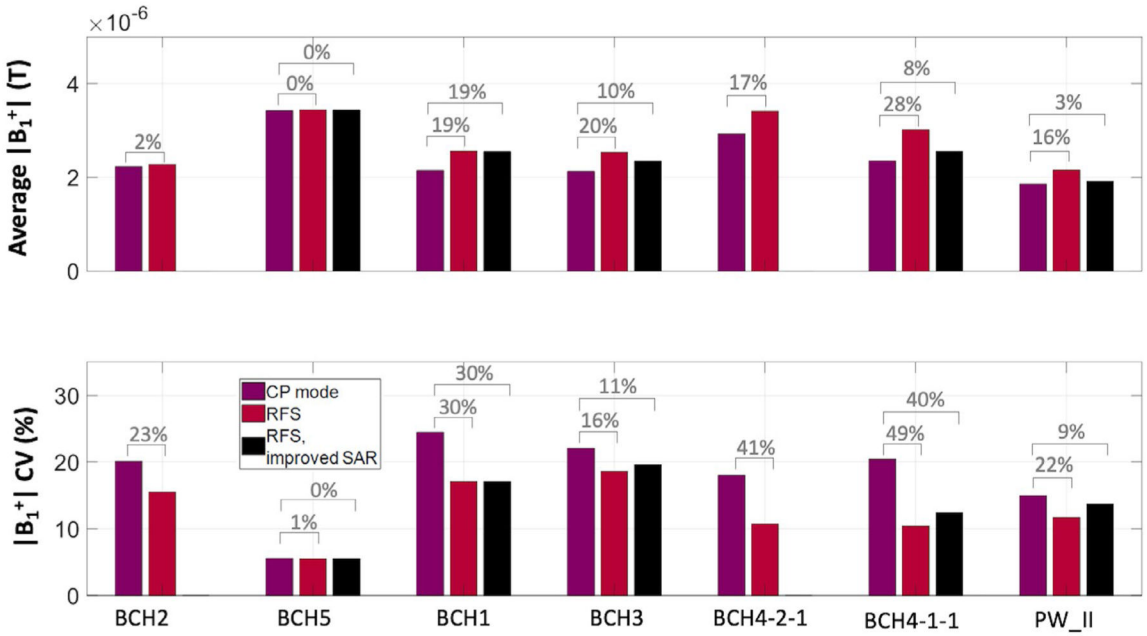

FIGURE 4.

Average and coefficient of variation (CV) of the transmit field magnitude ($|B_1^+|$) inside the fetus across different body models. CP mode: circularly polarized birdcage mode, RFS: optimal RF shim setting for average $|B_1^+|$ or $|B_1^+|$ CV with no SAR restrictions (red triangle or star in Figure 2), RFS, improved SAR: optimal RF shim setting for average $|B_1^+|$ or $|B_1^+|$ CV that also improves maternal and fetal SAR compared with CP mode of the corresponding model (black triangle or star in Figure 2). The percentages of improvement in average $|B_1^+|$ and $|B_1^+|$ CV when using RF shimming compared with CP mode are noted above the bar graphs

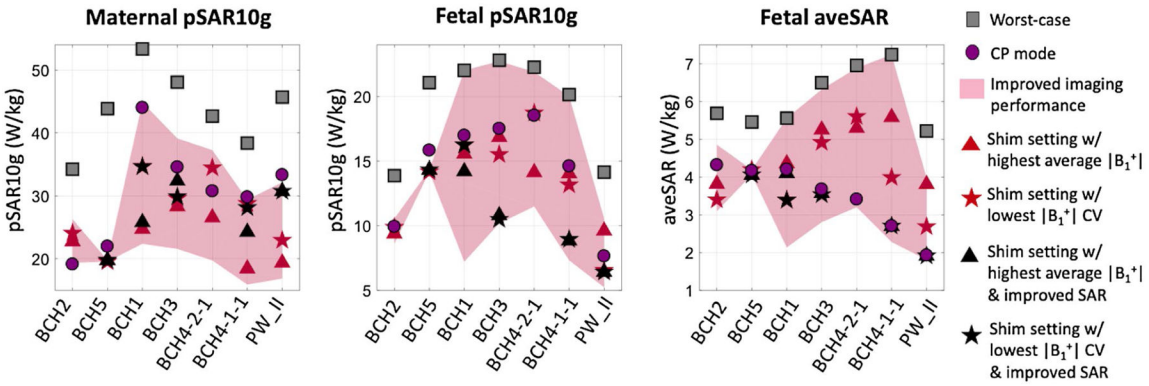

FIGURE 5.

Comparison of maternal and fetal peak local SAR (pSAR10g) and fetal average SAR (aveSAR) for different RF shim settings across various body models. Worst-case: RF shim setting that maximizes an individual SAR metric, CP mode: circularly polarized birdcage mode, improved imaging performance: both average $|B_1^+|$ and $|B_1^+|$ coefficient of variation (CV) is improved compared with CP mode, improved SAR: all three SAR metrics are less than the CP mode values of the corresponding model

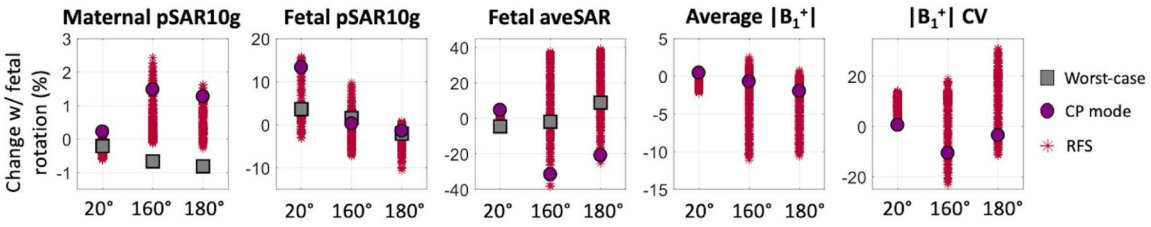

FIGURE 6.

Effect of fetal rotation by 20° (BCH4-2-2), 160° (BCH4-2-3), and 180° (BCH4-2-4) inside the uterus on maternal and fetal peak local SAR (pSAR10g), fetal average SAR (aveSAR), average $|B_1^+|$ and $|B_1^+|$ coefficients of variation (CV) for body model BCH4-2-1. Worst-case: RF shim setting that maximizes an individual SAR metric, CP mode: circularly polarized birdcage mode, RFS: RF shim settings that improve imaging performance in any of the four models BCH4-2-1, BCH4-2-2, BCH4-2-3, and BCH4-2-4

TABLE 1

The effect of tissue detail and dielectric properties on maternal and fetal peak local SAR and fetal average SAR for circularly polarized birdcage mode, RF shim settings which improve imaging performance and the worst-case shim settings

	No. of maternal tissues	No. of fetal tissues	Amniotic fluid properties	Fetal tissue properties	Maternal pSAR10g (W/kg)			Fetal pSAR10g (W/kg)			Fetal aveSAR (W/kg)		
					CP	RFS	WC	CP	RFS	WC	CP	RFS	WC
Murbach et al.[11]	>70	17	CSF	Adult	29.6 (−8%)	NA	39.9 (−10%)	7.4 (3%)	NA	21.3 (25%)	1.1 (−35%)	NA	2.8 (−39%)
This study	>70	17	CSF	Adult	32.5 (0%)	16.5–32.2 (0%–l%)	44.1 (0%)	8.6 (18%)	6.3–19.5 (−9% to 34%)	23.1 (35%)	1.2 (−29%)	1.1–2.9 (−34% to −29%)	3.2 (−31%)
	>70	17	CSF	Age adjusted	32.5 (1%)	16.3–32.3 (−1%to 1%)	44.3 (0%)	8.0 (11%)	6.0–16.5 (3%–14%)	18.9 (11%)	1.5 (−10%)	1.4–3.8 (−11% to −10%)	4.2 (−10%)
	>70	**17**	**Peyman et al.**[34]	**Age adjusted**	**32.3**	**16.5–32.2**	**44.2**	**7.2**	**5.4–15.3**	**17.1**	**1.7**	**1.5–4.2**	**4.6**
	>70	2	Peyman et al.[34]	Age adjusted	32.6 (1%)	16.1–32.5 (−3% to 2%)	44.3 (0%)	7.8 (7%)	5.5–13.1 (−18% to 9%)	15.0 (−12%)	2.1 (24%)	2.0–5.1 (19% −25%)	5.5 (19%)
	25	2	Peyman et al.[34]	Age adjusted	33.3 (3%)	16.8–33.3 (−4% to 8%)	45.7 (4%)	7.6 (6%)	5.2–12.3 (−22% to 7%)	14.2 (−17%)	1.9 (13%)	1.8–4.7 (11% −14%)	5.2 (12%)

Note: The RFS values report SAR metrics within the improved imaging performance region and are listed as a range from lowest to highest SAR metric in this region. The first row lists the findings of Murbach et al.,[11] who modeled a different body coil than this study. The second row reports SAR values found in this study with the same tissue property assignments as Murbach et al.[11] Subsequent rows report modifications to the PW_II model. Percentage values in parenthesis show the change in SAR values with respect to those in row 4 (in bold type), which presents the most-detailed model with the most realistic tissue properties.

Abbreviations: aveSAR, average SAR; CP, circularly polarized birdcage mode; CSF, cerebrospinal fluid; NA, not applicable; pSAR10g, 10g averaged peak local SAR; PW_II, pregnant woman II; RFS, radiofrequency shimming; SAR, specific absorption rate; WC, worst-case shim settings.